USRA Work Term Report
The Hard Square Constraint

Arman Raina Adrian She
Supervisors: Dr. Brian Marcus and Dr. Andrew Rechnitzer at UBC Math Department

Submitted September 9 2016

Contents

List of Figures

List of Tables

List of Notation

Notation	Explanation
$\mathcal{B}_{a,b,c}$	Set of hard square configurations on a $a \times b \times c$ broken box
$\mathcal{B}^0_{a,b,c}$	Subset of $\mathcal{B}_{a,b,c}$ compatible with checkboard with 0s bordering origin
$\mathcal{B}^1_{a,b,c}$	Subset of $\mathcal{B}_{a,b,c}$ compatible with checkboard with 1s bordering origin
$\mathcal{BR}_n$	Set of broken rhombii of radius n
$\mathcal{R}_{m,n}$	Set of hard square configurations on a $m \times n$ box
$\mathcal{RH}_n$	Set of hard square configurations on a radius n rhombus
B_p	Transfer matrix for hard square cylindrical sequences of length p and weight 1
$B_{p,z}$	Transfer matrix for hard square cylindrical sequences of length p and weight z
c_n	Set of all binary sequences of length n with no adjacent 1s
d_n	Set of all circular binary sequences of length n with no adjacent 1s
T_p	Transfer matrix for hard squares sequences of length p and weight 1
$T_{p,z}$	Transfer matrix for hard squares sequences of length p and weight z
Λ_p	Dominant eigenvalue of T_p
$\Lambda_{p,z}$	Dominant eigenvalue of $T_{p,z}$
η	Hard square constant
ξ_p	Dominant eigenvalue of B_p
$\xi_{p,z}$	Dominant eigenvalue of $B_{p,z}$
$A(z)$	Corner pressure function
$P_{f,C,n}(z)$	Probability function of configuration C on $n \cdot n$ square
$P_{f,\mathcal{B}}(z)$	Limiting probability function of broken box origin = 0 for free boundary
$P^e_{f,\mathcal{B}}(z)$	Limiting probability function of even broken box = 0 for free boundary
$P^o_{f,\mathcal{B}}(z)$	Limiting probability function of odd broken box origin = 0 for free boundary
$P_{c,\mathcal{B}}(z)$	Limiting probability function of broken box origin = 1 for checkerboard boundary
$Z_{m,n}(z)$	Partition function for a $m \times n$ box
$Z_{a,b,c}(z)$	Partition function for a $a \times b \times c$ broken box
$Z^0_{a,b,c}(z)$	Partition function for a $a \times b \times c$ broken box with checkerboard boundary (origin bordering 0)
$Z^1_{a,b,c}(z)$	Partition function for a $a \times b \times c$ broken box with checkerboard boundary (origin bordering 1)
$Z_{n,\mathcal{BR}}(z)$	Partition function for a radius n Broken Rhombus
$\gamma(z)$	Inverse of $P_{c,\mathcal{B}}(z)$
$\kappa(z)$	Free energy function
$\rho(z)$	Surface pressure function

Introduction

Consider the set of binary strings of length n with no adjacent "1" s. We will denote this set by c_n, and the size of this set by $||c_n||$. For example:

$$\begin{aligned} c_1 &\equiv \{0, 1\} && ||c_1|| = 2 \\ c_2 &\equiv \{00, 01, 10\} && ||c_2|| = 3 \\ c_3 &\equiv \{000, 001, 010, 100, 101\} && ||c_3|| = 5 \\ c_4 &\equiv \{0000, 0001, 0010, 0100, 0101, 1000, 1001, 1010\} && ||c_4|| = 8 \end{aligned}$$

Note that $c_\infty = X$ denotes a set of infinite sequences. If we view $||c_n|| \equiv (2, 3, 5, 8 \dots)$ as a sequence we soon realize that this $||c_n||$ is in fact the **Fibonacci sequence**. The quantity which we are most interested in computing is known as the **growth rate** of c_n, defined as $\lim_{n\to\infty} ||c_n||^{\frac{1}{n}}$. Strings in c_n may be constructed by recording the label vertexes reached in a path of length $n-1$ on the graph G in Figure 1.

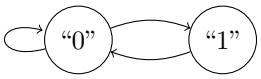

Figure 1: A graph G whose paths construct sequences in c_n

It is known that the growth rate of c_n is the largest eigenvalue of the adjacency matrix of G, namely $\frac{1+\sqrt{5}}{2}$. Hence, the set X is known as the **golden mean shift**. The logarithm is the growth rate is known as the (topological) **entropy** of the shift. Entropy, which for this system is about 0.69, represents the average number of bits of information per symbol in an infinite sequence. Quantities such as entropy and the growth rate are important because of their physical meanings. For instance, the golden mean shift can be thought of as a model of binary information storage on a magnetic tape. A change in magnetic field induces a current in the reader, generally represented by a "1", while no current is represented by a "0". If the reader encounters consecutive changes in magnetic field, it might erroneously interpret it as a an absence of change in magnetic field. This is known as intersymbol interference. One way to avoid such errors is to construct a code to convert unconstrained "information" strings into a set of constrained "storage" strings in c_n without consecutive "1"s, each of which representing an unconstrained string. Thus entropy is thus a measure of the maximum efficiency of such a code. Additionally, this entropy can be understood as a limiting conditional entropy representing the amount of choice one has when choosing a symbol to extend a valid sequence in X by one symbol.

The growth rate (and entropy) of a large class of 1-dimensional constraints, that is sets of sequences over a particular alphabet with local constraints, can be analyzed much like the golden

mean constraint by converting the constraint into a graph G' and finding the dominant eigenvalue in the adjacency matrix of G'. These are known as as **sofic shifts** and much of the theory behind them is detailed in [1].

However, computation of growth rates in higher dimensions remains unsolved. The two-dimensional analogue of the golden mean shift forbids adjacent 1s horizontally or vertically in a binary two-dimensional $m \times n$ array. This is known as the **hard square constraint**.

$$\begin{bmatrix} 0 & 1 & 1 \\ 1 & 0 & 0 \\ 1 & 0 & 1 \end{bmatrix} \quad \begin{bmatrix} 0 & 1 & 0 \\ 1 & 0 & 1 \\ 0 & 1 & 0 \end{bmatrix}$$

Figure 2: The array on the left is invalid, while the one on the right is valid

The analogue of the growth rate, also known as the **hard square constant** η is defined as

$$\eta = \lim_{m,n\to\infty} f_{m,n}^{\frac{1}{mn}} \tag{1}$$

where $f_{m,n}$ is the number of $m \times n$ arrays obeying the hard square constraint. A closed-form expression for η remains an open question. However, there are a number of techniques based on linear algebra, detailed in Section 2.1 of the Discussion, which have obtained good rigorous approximations of η. Re-implementation of these methods formed the initial part of the authors' summer research.

The initial motivation for investigating the hard square constraint came from statistical mechanics. In this context, "0" represents the absence of an atom whereas "1" represents the presence of an atom. The hard square constraint is imposed since atoms cannot be too close to each other as there is a repelling force between them. Hard square configurations can then be weighted, where a configuration τ is given a weight $z^{(\tau)}$ where $1(\tau)$ is the number of 1s in τ and z is a real-valued parameter. Such a weight denotes the energy of the configuration τ. Then, the total weight of configurations is known as the **partition function**, defined as:

$$Z_{mn}(z) = \sum_{\tau \in \mathcal{R}_{m,n}} z^{\mathbb{1}(\tau)} \tag{2}$$

where $\mathcal{R}_{m,n}$ denotes the set of all $m \times n$ hard square configurations. Notice that this sum is dominated by configurations with a high-density of "atoms" for high values of z and a low density for low values of z, mirroring the phases of crystal and gas respectively. As such, the parameter z can be viewed as inversely related to the temperature of the system.

$$\begin{bmatrix} 0 & 0 & 0 & 0 \\ 0 & 0 & 0 & 0 \\ 0 & 0 & 1 & 0 \\ 0 & 0 & 0 & 0 \end{bmatrix} \quad \begin{bmatrix} 0 & 1 & 0 & 1 \\ 1 & 0 & 1 & 0 \\ 0 & 1 & 0 & 1 \\ 1 & 0 & 0 & 0 \end{bmatrix}$$

Figure 3: The array on the left models a gas, while the one on the right models a solid

The **free energy** $\kappa(z)$ is then the analogue of the hard square constant when hard square configurations are weighted, defined as

$$\kappa(z) = \lim_{m,n\to\infty} Z_{mn}(z)^{\frac{1}{mn}} = \lim_{n\to\infty} Z_{nn}(z)^{\frac{1}{n^2}} \tag{3}$$

Note that $\eta = \kappa(1)$ since $Z_{mn}(1) = f_{m,n}$ counts the number of configurations on a $m \times n$ box. There are a number of ways to compute $\kappa(z)$, as detailed in Sections 2.2-2.7. These methods include exploring hard square configurations on shapes related to squares, numeric methods using linear algebra, or analytical methods using series. The bulk of this summer project was devoted in implementing such methods and analyzing their performance.

There are a number of quantities of interest related to $\kappa(z)$. Firstly, there are a number of "phase transitions" in $\kappa(z)$, which mathematically, are discontinuities in its derivative. One phase transition conjectured by Baxter [2] is at $z_c = 3.7962 \pm 0.0001$. Physically, this means that the hard square configurations shift from being more like a gas to being more like a crystal when activity z is beyond z_c. This significance of this quantity is explored in Sections 2.2 and 2.7.

Furthermore, if $\kappa(z)$ represents the "bulk" behaviour of a hard square configuration, then there need to be additional terms which represent the behaviour at its sides and corners. Such quantities and their significance are explored in Sections 2.6 and 2.7.

Summary

We propose that a number of quantities are related to the free energy $\kappa(z)$ derived from the hard square partition function. For instance, an $a \times b \times c$ broken box consists of the set of sites on an $a \times b$ rectangle next to be an $(a+1) \times c$ rectangle. We may impose free or checkboard boundary conditions on such a rectangle, as illustrated below:

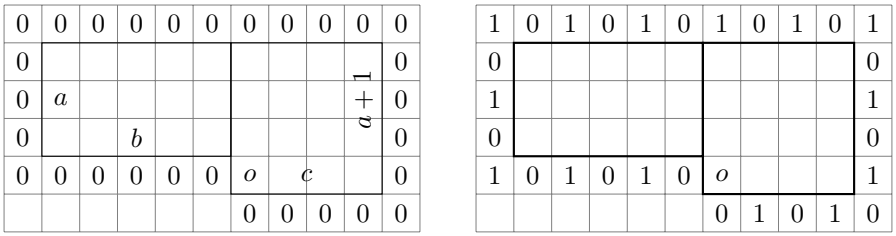

Figure 4: Broken boxes with free boundary condition (left) and checkboard boundary condition (right) with origin marked at o

Given free boundary conditions, we found that the limiting probability $P_{f,\mathcal{B}}(z)$ that the origin is zero as the dimensions a, b, c get large does not exist for large z. However, two subsequences over lattices with odd and even number of sites respectively have limits $P^e_{f,\mathcal{B}}(z)$ and $P^o_{f,\mathcal{B}}(z)$. We propose that

Conjecture 1. For all $z > 0$, $\kappa(z) = \frac{1}{\sqrt{P^e_{f,\mathcal{B}}(z) P^o_{f,\mathcal{B}}(z)}}$.

This extends a known theorem that $\kappa(z) = \frac{1}{P_{f,\mathcal{B}}(z)}$ for sufficiently small z, as the odd and even subsequences yield the same limit when z is small.

Given checkboard boundary conditions, we found that the limiting probability $P_{c,\mathcal{B}}(z)$ that the origin is one as dimensions a, b, c get large is related to $\kappa(z)$ as follows:

Conjecture 2. For all $z > 0$, $\kappa(z) = \sqrt{\frac{z}{P_{c,\mathcal{B}}(z)}}$

Conjecture 2 is known for $z < 2.48$ and $z > 468$ by [10], but our computations seem to suggest that it holds for all $z > 0$. Evidence from series expansions of $\kappa(z)$ supports the conjecture in addition to computated approximations of $P_{c,\mathcal{B}}(z)$.

Finally, we propose that $\kappa(z)$ is the limiting probability of seeing a 0 on a rhombus R_n as n gets large. A rhombus is a ball from a chosen origin point which are less than or equal to a distance n away in the taxicab, or graph metric. We find that some results for rhombii are analogous to results to broken boxes, particularly that the Conjectures 1 and 2 hold for rhombii if the probabilities on boxes are replaced by probabilities on rhombii.

Discussion

1 Materials

This project made heavy use of numerical methods. The main languages used were Octave and C++. Octave is an open-source alternative to Matlab. Octave was used because of its efficient matrix multiplication implementation and its graphics capabilities. In addition, since there are many syntactical shortcuts for dealing with lists, and the language handles memory internally, one can write correct, readable code quite fast. C++ was used as there are advantages for having more control over memory, when memory becomes scarce. Additionally, C++ can be a lot faster than Octave especially when using more customized operations. A C++ package that was occasionally used was Eigen, which includes efficient, basic matrix-vector operations. However, since we use numerical methods, our accuracy is limited to the accuracy of the "double" type in hardware. Extra steps can be taken in the code, in the future, to implement arbitrary decimal place floating point precision.

The code is available at `https://github.com/AdrianShe/coding-theory-usra`

2 Methods and Results

2.1 Eigenvalue Methods

As defined in the Introduction, the hard square constant η is

$$\eta = \lim_{m,n\to\infty} f_{m,n}^{\frac{1}{mn}} \tag{1.4}$$

where $f_{m,n}$ is the number of $m \times n$ binary arrays with no adjacent 1s in each row or column. There are a number of bounds for η based on techniques in linear algebra. A basic tool that we need to define behind these techniques is a special type of adjacency matrix known as the transfer matrix. Recall that as defined in the introduction, c_n is set of binary sequences of length n containing no adjacent "1"s. We may order sequences in c_n by treating each sequence as a binary number. Two sequences i, j are **compatible** if they do not have any "1"s in a common position. Then, we may define a directed graph G_n on the set c_n by declaring that there is an edge between compatible sequences.

$$\begin{bmatrix}1\\0\\1\\0\end{bmatrix}\quad\begin{bmatrix}0\\0\\1\\0\end{bmatrix}\qquad\begin{bmatrix}1\\0\\1\\0\end{bmatrix}\quad\begin{bmatrix}0\\1\\0\\1\end{bmatrix}$$

Figure 1.5: Sequences with (left) and without (right) "1"s in a common position

Definition 1. The matrix T_p is a symmetric $F_{p+2} \times F_{p+2}$ matrix which is the adjacency matrix of G_p.

For instance, the following illustrates G_3 and T_3.

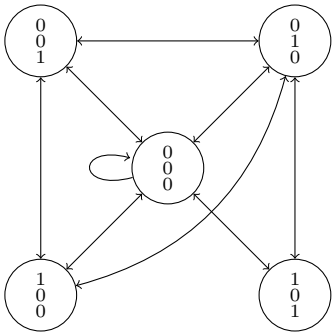

$$T_3 = \begin{bmatrix}1&1&1&1&1\\1&0&1&1&0\\1&1&0&1&1\\1&1&1&0&0\\1&0&1&0&0\end{bmatrix}$$

Figure 1.6: Graph and Matrix for T_3

Properties of the graph are related to the properties of the matrix. Recording the vertexes reached on a path of length n through G_p represents a hard square configuration of dimension $p \times (n+1)$. The sum of entries in T_p^n count the number of $p \times n + 1$ hard squares. Furthermore, the dominant eigenvalue of T_p, denoted by Λ_p is the growth rate for a hard square system of fixed width p. When the width p is fixed, the system becomes essentially one-dimensional since the system is the set of sequences with an alphabet in c_n, with some constraints on which symbols are allowed to be adjacent. In the case $p = 3$, Λ_3 is the largest root of $x^4 - 2x^3 - 6x^2 + 1 = 0$, which means that $\Lambda_3 = 3.6313812604036....$

Note that we may rewrite 1.4 as

$$\eta = \lim_{m,n\to\infty} f_{m,n}^{\frac{1}{mn}} = \lim_{m\to\infty} \Lambda_m^{\frac{1}{m}} \tag{1.5}$$

Although $\Lambda_m^{\frac{1}{m}}$ in theory, can be evaluated for each m to obtain a value for η, the limit in 1.5 converges slowly as we will see in the following numeric computations. Furthermore, the size of the matrices T_p grows exponentially and hence it becomes infeasible to find the eigenvalues of T_p except for small or moderate p.

Next, let d_n denote the set of sequences in c_n where the first and last positions do not contain a 1 simultaneously. By case analysis, $||d_n|| = F_{n+1} + F_{n-1}$ where F_i is the i^{th} Fibonacci number. For instance $101 \in c_3$ but $101 \notin d_3$. We may define a directed graph H_n on d_n by declaring that there is an edge between compatible sequences.

Definition 2. The matrix B_p is a symmetric $(F_{p+1} + F_{p-1}) \times (F_{p+1} + F_{p-1})$ matrix which is the adjacency matrix of H_p.

Concretely, the following figure illustrates B_3

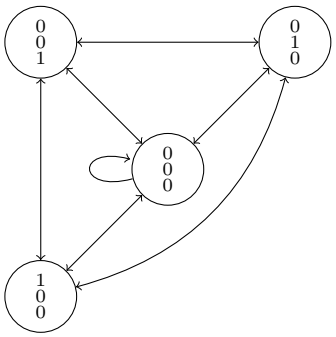

$$B_3 = \begin{bmatrix} 1 & 1 & 1 & 1 \\ 1 & 0 & 1 & 1 \\ 1 & 1 & 0 & 1 \\ 1 & 1 & 1 & 0 \end{bmatrix}$$

Figure 1.7: Graph and Matrix for B_3

The eigenvalue ξ_p is the dominant eigenvalue of B_p. In this case ξ_3 is the largest root of $x^4 - x^3 - 6x^2 - 5x - 1$, namely 3.302775637731995.... Existence of eigenvalues Λ_p, ξ_p of T_p, B_p respectively is given by the Perron-Frobenius theorem guaranteeing existence of a dominant positive eigenvalue for every non-negative matrix.

Now we state a number of bounds for η based on eigenvalues Λ_p, ξ_p.

First, Engel in [4] obtained the following bound on η:

Theorem 1 (Engel Bound)**.** For all $k, l \geq 1$:

$$\frac{\Lambda_{2k}}{\Lambda_{2k-1}} \leq \eta \leq \Lambda_l^{\frac{1}{l}} \tag{1.6}$$

Based on the Rayleigh quotient and trace bound for symmetric matrices, Calkin and Wilf in [3] gave the following bound on η:

Theorem 2 (Calkin-Wilf Bound)**.** For every $p, q, r \geq 1$:

$$\left(\frac{\Lambda_{p+2q+1}}{\Lambda_{2q+1}}\right)^{\frac{1}{p}} \leq \eta \leq \xi_{2r}^{\frac{1}{2r}} \tag{1.7}$$

Friedland in [5] obtained the following lower bound on η based on symmetry of the matrix B_p:

Theorem 3 (Friedland Bound)**.** For every $p, q \geq 1$:

$$\left(\frac{\xi_{p+2q}}{\xi_{2q}}\right)^{\frac{1}{p}} \leq \eta \tag{1.8}$$

We implemented code to compute eigenvalues Λ_p, ξ_p for all $p \leq 20$, and hence were able to compute bounds on η based on 1.6, 1.7, and 1.8. The following table states our most accurate bounds based on the above theorems.

Method	Lower Bound	Upper Bound	Exact Digits of η
Engel	$\frac{\Lambda_{20}}{\Lambda_{19}} = 1.50304808247534...$	$\Lambda_{20}^{\frac{1}{20}} = 1.50809590168225...$	$\eta = 1.50...$
Calkin-Wilf	$(\frac{\Lambda_{19}}{\Lambda_{17}})^{\frac{1}{2}} = 1.50304808247533...$	$\xi_{20}^{\frac{1}{20}} = 1.50304808490576...$	$\eta = 1.50304808...$
Friedland	$(\frac{\xi_{20}}{\xi_{18}})^{\frac{1}{2}} = 1.50304799483443...$	N/A	$\eta = 1.50304....$

Table 1.1: Bounds for η based on Eigenvalues

We may also use eigenvalues Λ_p for $p \leq 28$ and eigenvalues ξ_p for $p \leq 36$, computed in [5] to obtain additional bounds.

Method	Lower Bound	Upper Bound	Exact Digits of η
Engel	$\frac{\Lambda_{28}}{\Lambda_{27}} = 1.50304808247533...$	$\Lambda_{28}^{\frac{1}{28}} = 1.50665194025740...$	$\eta = 1.50...$
Calkin-Wilf	$(\frac{\Lambda_{27}}{\Lambda_{25}})^{\frac{1}{2}} = 1.50304808247533...$	$\xi_{36}^{\frac{1}{36}} = 1.50304808247534...$	$\eta = 1.5030480824753...$
Friedland	$(\frac{\xi_{36}}{\xi_{34}})^{\frac{1}{2}} = 1.50304808247485...$	N/A	$\eta = 1.50304808247....$

Table 1.2: Bounds for η based on Friedland's Eigenvalues

Finally, based on a different "corner transfer matrix" approach, Chan and Rechnitzer computed in [6] and [7] that

$$\eta = 1.503048082475332264...$$

This value of η was used in validating some of our work.

The Calkin-Wilf bound in particular can be used to give rigorous bounds for $\kappa(z)$. As in the introduction, $\kappa(z)$ is defined as

$$\kappa(z) = \lim_{n\to\infty} Z_{nn}(z)^{\frac{1}{n^2}} \tag{1.9}$$

where $Z_{nn}(z)$ is the partition function over an $n \times n$ box. The values of $Z_{nn}(z)$ are computed using a modified transfer matrix. That is,

$$Z_{nn}(z) = (\mathbf{1}, T_{n,z}^{n-1}\mathbf{v}) = \sum_{\tau\in\mathcal{R}_{n,n}} z^{1(\tau)}$$

where $(\cdot,\cdot)$ is the dot product, $1(\tau)$ denotes the number of 1s in configuration τ, $\mathbf{v}$ is a vector of length $|\mathcal{S}_n|$ wherein the i^{th} component of $\mathbf{v}$ is $z^{1(i)}$ where $1(i)$ is the number of 1s in sequence i , $\mathbf{1}$ is a vector of ones of length $||c_n||$ and $T_{n,z}$ is a square matrix indexed by $||c_n||$ states such that $(T_{n,z})_{ij} = \begin{cases} z^{1(i)} & i,j \text{ compatible} \\ 0 & \text{otherwise} \end{cases}$.

In general, the matrix $T_{n,z}$ is not symmetric, but Calkin-Wilf methods can be applied since $T_{n,z}$ is similar to a symmetric matrix. Similar matrices have the same set of eigenvalues.

Theorem 4. Let D_n be a diagonal matrix indexed by $\mathcal{S}_n$ where $D_{ii} = z^{\frac{1(i)}{2}}$ and $1(i)$ is the number of 1s in sequence i. Then for every z, $D_n^{-1}T_{n,z}D_n$ is symmetric.

Hence, the Calkin-Wilf bound can be modified to bound $\kappa(z)$:

Theorem 5 (Modified Calkin-Wilf Bound)**.** Suppose $\Lambda_{p,z}$ is the dominant eigenvalue $T_{p,z}$ and $\xi_{p,z}$ is the dominant eigenvalue of $B_{p,z}$. Then for all $p, q, r \geq 1$ and $z > 0$:

$$\Big(\frac{\Lambda_{p+2q+1,z}}{\Lambda_{2q+1,z}}\Big)^{\frac{1}{p}} \leq \kappa(z) \leq \xi_{2r,z}^{\frac{1}{2r}} \tag{1.10}$$

We tried this for the case $z = 10$, giving us a bound of

$$\frac{\Lambda_{20,10}}{\Lambda_{19,10}} = 3.31801717090024... = \kappa(10) = \xi_{20,10}^{\frac{1}{20}} = 3.31804721565178...$$

Hence $\kappa(10) = 3.3180...$

2.2 Broken Box- Free Boundary

In the previous section we built hard square configurations one column at a time using the transfer matrix method. In this section we will proceed more incrementally, considering what happens when we build a large square, one site at a time. In the one dimensional case, the growth rate in number of configurations was related to the probabilities that the next site added was 0 or 1.

We observe a similar phenomenon in the two dimensional case. We will thus consider several probabilities whose reciprocals appear to converge to $\kappa(z)$.

Definition 3. The set of $a \times b \times c$ broken box configurations, $\mathcal{B}_{a,b,c}$, includes all possible hard square configurations composed of a $a \times b$ rectangle adjacent to a $a+1 \times c$ rectangle, as indicated in the figure below:

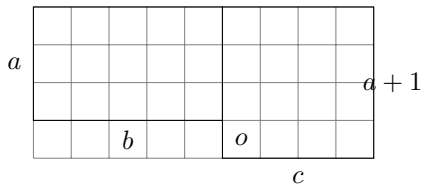

Figure 1.8: Illustration of Broken Box

The square marked with o is known as the origin. Here $a = 3$, $b = 5$, $c = 4$. Based on the set $\mathcal{B}_{a,b,c}$, we may construct the broken box partition function $Z_{a,b,c}(z)$ as

$$Z_{a,b,c}(z) = \sum_{\tau \in \mathcal{B}_{a,b,c}} z^{\mathbb{1}(\tau)}$$

First we consider the limiting probability of the origin of the broken box, $P_{f,\mathcal{B}}(z)$, being assigned a 0 for each different energy z. This may be computed from the partition function since

$$P_{f,\mathcal{B}}(z) = \lim_{a,b,c \to \infty} \frac{Z_{a,b+1,c-1}(z)}{Z_{a,b,c}(z)} \tag{1.11}$$

We approximated $P_{f,\mathcal{B}}(z)$ by computing $Z_{a,b,c}(z)$ for finite a, b, c using a modified transfer matrix method, then computing the ratio in 1.11. For $z = 1$, the reciprocal of the probability appears to be approaching $\eta = \kappa(1)$. Using a $17 \times 40 \times 40$ box yields

$$\frac{1}{P_{f,\mathcal{B}(1)}} \approx 1.503048082475322$$

, which η is correct up to 13 decimal places. If a $17 \times 41 \times 41$ box is used, the approximation is correct to 14 decimal places.

In fact, as mentioned in [11]:

Theorem 6. Suppose $0 < z < 2.48$, then

$$\frac{1}{P_{f,\mathcal{B}}(z)} = \kappa(z)$$

We then computed approximations to $\frac{1}{P_{f,\mathcal{B}}(z)}$ for z outside the specified range. Outside this range, it is not known whether the limit $P_{f,\mathcal{B}}(z)$ converges. In fact the data suggests two different limits, $P^e_{f,\mathcal{B}}(z)$ and $P^e_{f,\mathcal{B}}(z)$, based on the parity on the number of sites on the Broken Box as demonstrated below.

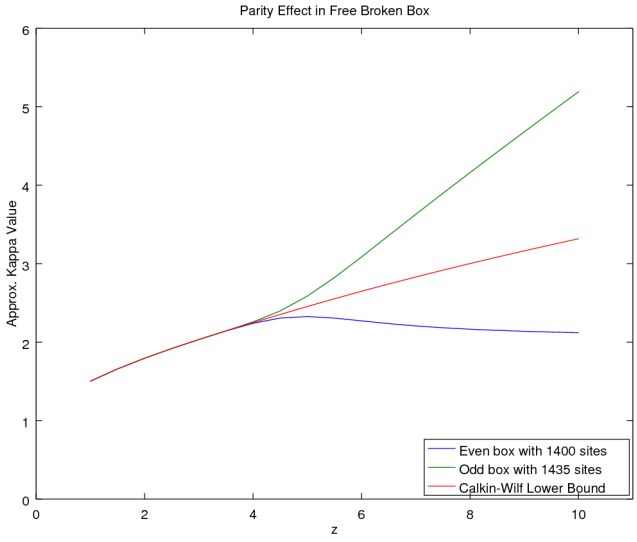

Figure 1.9: The parity effect on the number of sites

However, if we compute the geometric mean of the two parities, it appears to approach $\kappa(z)$.

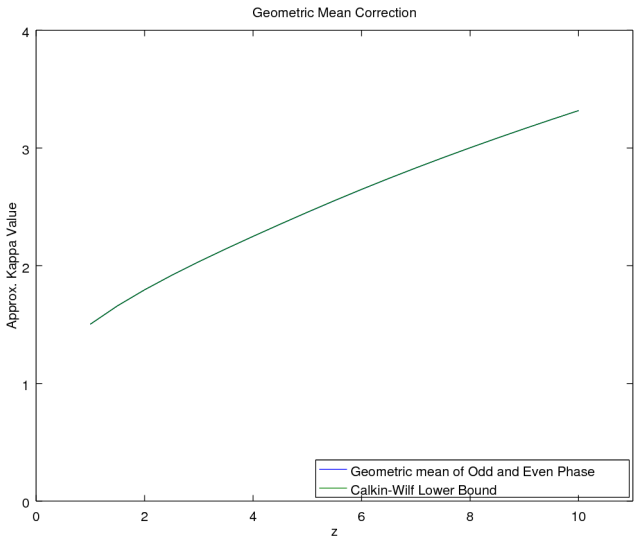

Figure 1.10: The mean appears to be consistent with Calkin and Wilf

Based on the computational experiment, we make the following conjecture:

Conjecture 1. Let $z > 0$, then

$$\frac{1}{\sqrt{P^e_{f,\mathcal{B}}(z) \cdot P^o_{f,\mathcal{B}}(z)}} = \kappa(z)$$

This reduces to Theorem 6 when z is sufficiently small as the odd and even probabilities converge to the same limit.

2.3 Broken Box - Checkboard Boundary

If we think more carefully about the parity effect observed in the previous section, we realize that it is possibly because of the "free" boundary that we observe the parity effect for higher values of z. This is because for higher values of z, the configuration with the maximal number of 1's dominates. Since there is one more maximal configuration in a configuration with an even number of sites than an odd number of sites, we might expect to observe a parity effect.

In this section we will will attempt to eliminate the parity effect by altering the boundary to a sea of alternating 'checkerboard' 1's and 0's.

1	0	1	0	1	0	1	0	1	0	1
0										0
1										1
0										0
1	0	1	0	1	0	o				1
						0	1	0	1	0

Figure 1.11: The checkerboard boundary where the origin is marked with an o

Since there are two possible phases of boundary, we define two sets of configurations and two partition functions, depending on whether the origin is bordered by two 1's or two 0's.

Definition 4. $\mathcal{B}^0_{a,b,c}$ is the subset of configurations in $\mathcal{B}_{a,b,c}$ which are compatible with the checkerboard boundary condition where the origin is bordered by two 0s. $\mathcal{B}^1_{a,b,c}$ is the subset of $\mathcal{B}_{a,b,c}$ compatible with 1s bordering the origin.

The checkerboard broken box partition functions are defined similarly as

$$Z^0_{a,b,c} = \sum_{\tau \in B^0_{a,b,c}} z^{\mathbb{1}(\tau)} \, Z^1_{a,b,c} = \sum_{\tau \in B^1_{a,b,c}} z^{\mathbb{1}(\tau)} \tag{1.12}$$

We would like to consider the probability of the origin "continuing" the checkboard condition on its boundary. In the case where the origin is bordered by 1s, the origin is forced to be a 0 and hence the origin must continue the checkerboard boundary condition. Otherwise, when the origin is bordered by 0s, the origin may be 0 and 1 and to continue the checkboard, the origin should be 1. As in Section 2.2, we want to consider the limiting probability function $P_{c,\mathcal{B}}(z)$ for this event:

Definition 5.

$$P_{c,\mathcal{B}}(z) = \lim_{a,b,c\to\infty} \frac{\text{Weight of Configurations on } a\times b\times c \text{ box where origin} = 1}{\text{Total weight of } a\times b\times c \text{ box}} = 1 - \lim_{a,b,c\to\infty} \frac{Z^1_{a,b+1,c-1}(z)}{Z^0_{a,b,c}(z)}$$

Once again, we approximate this by computations for finite a, b, c using a modified transfer matrix method. However, in this case $z = 1$ using a $17 \times 40 \times 40$ box, we obtain

$$\frac{1}{P_{c,\mathcal{B}}(1)} \approx 2.25915093474208 \approx \eta^2$$

. The following theorem stated in [10] justifies this result:

Theorem 7. Let $z \in \mathbb{R}$ s.t. $0 < z < 2.48$ or $z > 468$, then

$$\sqrt{\frac{z}{P_{c,\mathcal{B}}(z)}} = \kappa(z)$$

We computed approximations to $\sqrt{\frac{z}{P_{c,\mathcal{B}}(z)}}$ for z outside the specified range, which is similar to what we did in Section 2.2. Outside this range, it is not known whether the limit in $\sqrt{\frac{z}{P_{c,\mathcal{B}}(z)}}$ converges. However, $\sqrt{\frac{z}{P_{c,\mathcal{B}}(z)}}$ does appear to converge to $\kappa(z)$ outside this range as well.

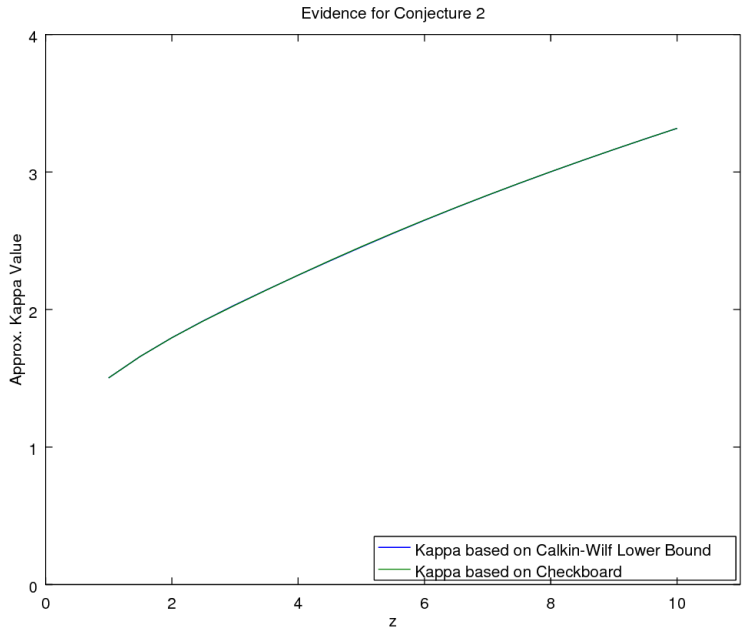

Figure 1.12: The approximation appears to converge to $\kappa(z)$

We thus state the following conjecture:

Conjecture 2. Let $z > 0$, then

$$\kappa(z) = \sqrt{\frac{z}{P_{c,\mathcal{B}}(z)}}$$

2.4 Heuristic

In this section we will provide some intuition as to why we believe Conjecture 1 in Section 2.2 and Conjecture 2 in Section 2.3 are true.

Suppose we have a configuration τ and activity z on the infinite square lattice $\mathbb{Z}^2$. We then carve out an $n \times n$ box from $\mathbb{Z}^2$. We define the boundary configuration ω as τ restricted to the set of sites outside the box.

We then consider the set of all allowable hard square configurations $\mathcal{C}_n^\omega$ that can be placed in the box with the boundary ω. Then, we consider the probability that an element σ of $\mathcal{C}_n^\omega$ can be chosen such that the τ can be reconstructed. That is, $\sigma \cup \omega = \tau$.

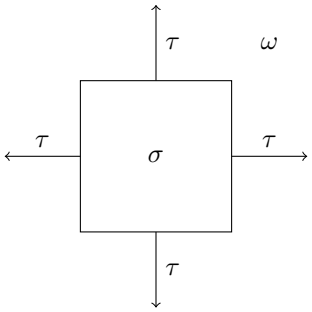

Figure 1.13: Illustration of where τ, ω, σ are placed

The element we need to choose will be called ν, which is τ restricted to the box. We may compute the probability that $\sigma = \nu$ in the cavity, $P^{\omega}_{\sigma=\nu}(z)$, by considering the weight which ν contributes to the partition function $Z^{\omega}_{nn}(z)$ over $\mathcal{C}^{\omega}_{n}$. Hence, we say that

$$P^{\omega}_{\sigma=\nu}(z) = \frac{\text{Weight of } \nu}{\text{Total Weight of } \mathcal{C}^{\omega}_{n}} = \frac{z^{\mathbb{1}(\nu)}}{Z^{\omega}_{nn}(z)} \tag{1.13}$$

Alternatively, we may label each cell of the box an $n \times n$ box by s_i moving from left to right, top to bottom. Let the symbol in the i^{th} site of configuration σ be denoted as σ_{s_i}.

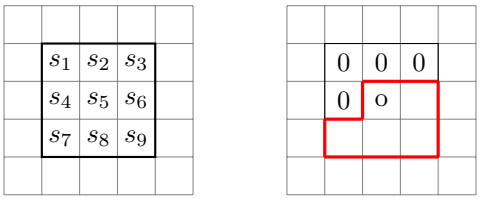

Figure 1.14: Illustration of Probability Computation

We can define $P^{\omega}_{\sigma=\nu}(z)$ as a product of the sitewise conditional probabilities. If $\sigma = \nu$, then every symbol in σ matches every symbol in ν and at the same position. Hence, by the definition of conditional probabilities, we may perform a decomposition since $P(A \cap B) = P(B|A)P(A)$ for events A, B . It is implied in 1.14 and 1.15 that the probabilities are a function of z and ω.

$$\begin{aligned} P(\sigma = \nu) &= P\left(\cap_{i=1}^{n^2}(\sigma_{s_i} = \nu_{s_i})\right) = P\left((\sigma_{s_1} = \nu_{s_1}) \cap \cap_{i=2}^{n^2}(\sigma_{s_i} = \nu_{s_i})\right) \\ &= P\left(\cap_{i=2}^{n^2}(\sigma_{s_i} = \nu_{s_i}) \mid \sigma_{s_1} = \nu_{s_1}\right) P(\sigma_{s_1} = \nu_{s_1}) \end{aligned} \tag{1.14}$$

In words, 1.14 means that the probability that σ and ν match is the probability that the first sites match multiplied by the probability the rest of the sites match, given that the first site

matches. We may repeat the decomposition 1.14 as follows:

$$\begin{aligned}
P(\sigma = \nu) &= P\left(\cap_{i=2}^{n^2}(\sigma_{s_i} = \nu_{s_i}) \mid \sigma_{s_1} = \nu_{s_1}\right) P(\sigma_{s_1} = \nu_{s_1}) \\
&= P\left(\cap_{i=3}^{n^2}(\sigma_{s_i} = \nu_{s_i}) \mid \sigma_{s_1} = \nu_{s_1} \cap \sigma_{s_2} = \nu_{s_2}\right) P(\sigma_{s_2} = \nu_{s_2} \mid \sigma_{s_1} = \nu_{s_1}) P(\sigma_{s_1} = \nu_{s_1}) \\
&= P\left(\cap_{i=4}^{n^2}(\sigma_{s_i} = \nu_{s_i}) \mid \cap_{i=1}^{3}(\sigma_{s_i} = \nu_{s_i})\right) P(\sigma_{s_3} = \nu_{s_3} \mid \cap_{i=1}^{2}(\sigma_{s_1} = \nu_{s_i})) \\
&\quad P(\sigma_{s_2} = \nu_{s_2} \mid \sigma_{s_1} = \nu_{s_1}) P(\sigma_{s_1} = \nu_{s_1}) \\
&= \prod_{i=1}^{n^2} P(\sigma_{s_i} = \nu_{s_i} \mid \cap_{j=1}^{i-1}(\sigma_{s_i} = \nu_{s_i}))
\end{aligned} \tag{1.15}$$

In order to compute the i^{th} term in 1.15, we consider the site s_i as part of an $n \times n$ box and fix the symbols in sites $\{s_1, ..., s_{i-1}\}$ to match $\{\nu_{s_1}, ..., \nu_{s_{i-1}}\}$. Then we consider all valid configurations $\mathcal{C}_{s_i}$ on sites $\{s_i, ..., s_{n^2}\}$ which can extend the configuration on $\{s_1, ..., s_{i-1}\}$ onto the full $n \times n$ box. The i^{th} probability term is then

$$\frac{\text{Energy of Configurations in } \mathcal{C}_{s_i} \text{ where } \sigma_{s_i} = \nu_{s_i}}{\text{Total Energy of Configurations in } \mathcal{C}_{s_i}}$$

. That is, in the i^{th} term, our condition is that all **past** sites from s_i match ν, and we compute from all possible **futures** the probability that s_i matches ν_{s_i}. Figure 1.14 illustrates computing the 5^{th} probability term on an 3×3 box when $\nu = 0^{\mathbb{Z}^2}$. Each term of the decomposition describes a "broken box" as outlined in Sections 2.2-2.3.

Now since 1.13 and 1.15 are different formulae for the same quantity, we may equate them.

$$\frac{z^{\mathbb{1}(\nu)}}{Z_{nn}^{\omega}(z)} = \prod_{i=1}^{n^2} P^{\omega}(\sigma_{s_i} = \nu_{s_i} \mid \cap_{j=1}^{i-1}(\sigma_{s_i} = \nu_{s_i}))(z) \tag{1.16}$$

Rearranging and taking n^2 roots yields

$$(Z_{nn}^{\omega}(z))^{\frac{1}{n^2}} = \Big(\frac{z^{\mathbb{1}(\nu)}}{\prod_{i=1}^{n^2} P^{\omega}(\sigma_{s_i} = \nu_{s_i} \mid \cap_{j=1}^{i-1}(\sigma_{s_i} = \nu_{s_i}))(z)}\Big)^{\frac{1}{n^2}} \tag{1.17}$$

Suppose we take the limit of 1.17 as $n \to \infty$. The following lemma indicates what the left hand side of 1.17 should be.

Lemma 1. For every boundary configuration ω:

$$\kappa(z) = \lim_{n \to \infty} (Z_{nn}^{\omega}(z))^{\frac{1}{n^2}}$$

Lemma 1 can be proven by "squeezing" the partition function $Z_{nn}^{\omega}(z)$ between partition functions $Z_{ii}^{\text{free}}(z)$ and $Z_{jj}^{\text{free}}(z)$ for appropriately chosen i, j. Informally this means padding the boundary configuration ω with "0"s on the inside and out.

Interpreting the right hand side of the equation as $n \to \infty$ by imposing $\tau = 0^{\mathbb{Z}^2}$, the free condition, or $\tau = (01)^{\mathbb{Z}^2}$, the checkerboard condition, yields the Conjectures 1 and 2, derived as follows.

Suppose $\tau = 0^{\mathbb{Z}^2}$. In this case $\mathbb{1}(\tau) = 0$. Firstly, we decompose the product in the denominator as follows:

$$\begin{aligned}\kappa(z) &= \lim_{n\to\infty}\left(\frac{1}{\prod_{i=1}^{n^2} P(\sigma_{s_i}=0 \mid \cap_{j=1}^{i-1}(\sigma_{s_i}=0))(z)}\right)^{\frac{1}{n^2}} \\ &= \lim_{n\to\infty}\left(\frac{1}{\prod\limits_{\text{odd sites i}} P(\sigma_{s_i}=0 \mid \cap_{j=1}^{i-1}(\sigma_{s_i}=0))(z)\cdot \prod\limits_{\text{even sites i}} P(\sigma_{s_i}=0 \mid \cap_{j=1}^{i-1}(\sigma_{s_i}=0))(z)}\right)^{\frac{1}{n^2}}\end{aligned} \tag{1.18}$$

We divided the product into a product over odd sites and a product over even sites because of parity effects. However, in each separate product, we expect that each individual term will be close their respective limiting probability functions, and also to each other when n is large. This is because these sites are all part of the "bulk" and remain unaffected by the boundary conditions. Hence, we may expect in the limit, each individual term will be the same and be equal to the limiting probability function. Denoting the odd and even limiting probability functions by $P^o_{f,\mathcal{B}}(z)$ and $P^e_{f,\mathcal{B}}(z)$ respectively and applying our heuristic in 1.18 yields our Conjecture 1. That is:

$$\begin{aligned}\kappa(z) &= \lim_{n\to\infty}\left(\frac{1}{\prod\limits_{\text{odd sites i}} P(\sigma_{s_i}=0 \mid \cap_{j=1}^{i-1}(\sigma_{s_i}=0))(z)\cdot \prod\limits_{\text{even sites i}} P(\sigma_{s_i}=0 \mid \cap_{j=1}^{i-1}(\sigma_{s_i}=0))(z)}\right)^{\frac{1}{n^2}} \\ &\approx \lim_{n\to\infty}\left(\frac{1}{(P^o_{f,\mathcal{B}}(z))^{\frac{n^2}{2}}\cdot(P^e_{f,\mathcal{B}}(z))^{\frac{n^2}{2}}}\right)^{\frac{1}{n^2}} \\ &= \lim_{n\to\infty}\left(\frac{1}{(P^o_{f,\mathcal{B}}(z))^{\frac{1}{2}}\cdot(P^e_{f,\mathcal{B}}(z))^{\frac{1}{2}}}\right) \\ &= \frac{1}{\sqrt{P^o_{f,\mathcal{B}}(z)\cdot P^e_{f,\mathcal{B}}(z)}}\end{aligned} \tag{1.19}$$

Now suppose that $\tau = (01)^{\mathbb{Z}^2}$. Here approximately half of sites will contain a 1 and approximately half of sites will contain a 0. Hence $z^{\mathbb{1}(\tau)} = z^{\frac{n^2}{2}}$. Similarly, we can decompose the product into sites with "0" and sites with a "1". In equations, this means that:

$$\kappa(z) = \lim_{n\to\infty}\left(\frac{z^{\frac{n^2}{2}}}{\prod\limits_{\text{odd sites i}} P(\sigma_{s_i}=0 \mid (\cap_{j=1}^{i-1}\sigma_{s_i}=01))(z)\cdot \prod\limits_{\text{even sites i}} P(\sigma_{s_i}=1 \mid (\cap_{j=1}^{i-1}\sigma_{s_i}=01))(z)}\right)^{\frac{1}{n^2}} \tag{1.20}$$

The limit of the numerator in 1.20 will be $\sqrt{z}$. Additionally, the product over odd sites will be 1 since those sites are forced to be "0" by the surrounding "1"s to the top and left. For sites

in which we can put a "1" (and are surrounded by "0"s), we will apply our heuristic. That is, we assume that each sitewise probability is the same in the limit and that the finite sitewise probability is the same as the limiting probability, we did in 1.18. Combining all these steps together yields Conjecture 2. That is,

$$\begin{aligned}
\kappa(z) &= \lim_{n\to\infty} \frac{\sqrt{z}}{1 \cdot \left(\prod_{\text{even sites i}} P(\sigma_{s_i} = 1 \mid (\cap_{j=1}^{i-1} \sigma_{s_i} = 01))(z) \right)^{\frac{1}{n^2}}} \\
&\approx \lim_{n\to\infty} \frac{\sqrt{z}}{1 \cdot (P_{c,\mathcal{B}}(z))^{\frac{n^2}{2} \cdot \frac{1}{n^2}}} \\
&= \lim_{n\to\infty} \frac{\sqrt{z}}{(P_{c,\mathcal{B}}(z))^{\frac{1}{2}}} \\
&= \sqrt{\frac{z}{P_{c,\mathcal{B}}(z)}}
\end{aligned} \tag{1.21}$$

Our heuristic, used in 1.19 and 1.21 that each conditional sitewise probability is about the same and is sufficiently close to the limiting probabilities can be made more rigorous for certain values of the activity. To make the heuristic more rigorous, we need to argue the effect of the imperfections of the boundary when an $n \times n$ box is placed in it "decays" rapidly enough such that we can consider the site-wise probabilities to be approximately the same, and also about the convergence rates of the sitewise probabilities on a finite lattice to the limiting probabilities. Strong spatial mixing, as described in [10] is one way of making our heuristic more rigorous and hence Conjectures 1 and 2 have been proven for the ranges of z in which this condition holds. More careful analysis or extensions of this technique may be useful in proving Conjectures 1 and 2 across all z for which we believe they are true.

2.5 Broken Rhombus

In the previous four sections we considered quantities defined on either a square or a subset of a rectangle (a broken box). A square is a ball in the maximum norm on the square lattice $\mathbb{Z}^2$. However, the hard square constraint itself is defined in terms of taxicab norm, that is the minimum number of edges needed to connect two points. In this section, we apply the techniques developed in Sections $2.2 - 2.3$ to a ball defined using the taxicab norm. Such a ball we call a **rhombus**. We will explore several probabilities on what we call the **broken rhombus**.

Definition 6. The set of **rhombii**, $\mathcal{RH}_n$, includes only configurations composed of all sites of taxicab distance n from the origin, such as the figure below:

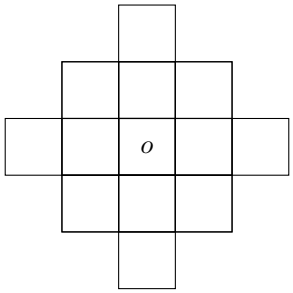

Figure 1.15: The site marked with o is the origin, $n = 2$.

Definition 7. The set of broken rhombii, $\mathcal{BR}_n$, includes only configurations composed of the subset of sites in $\mathcal{RH}_n$ in the upper right half of the rhombus. It can be constructed as follows:

- Start with the sites in $\mathcal{RH}_n$.
- Divide the Rhombus along a top-left to bottom-right diagonal through the origin.
- Drop all sites to the left or below the diagonal.
- All sites on the diagonal to the left of the origin are dropped while all sites on the diagonal to right are kept.

The figure below illustrates a broken rhombus where $n = 2$:

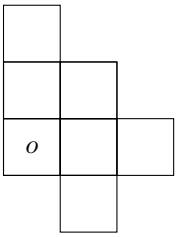

Figure 1.16: The broken rhombus

The site marked with o is the origin, $n = 2$.

First we consider the limiting probability of the origin being assigned a 0 under free boundary conditions, $P_{f,\mathcal{BR}}(z)$.

Once again, we approximate this by computations for finite n using a modified transfer matrix method and for $z = 1$, the reciprocal of the probability appears to be approaching $\kappa(1)$. For example, with $n = 14$ the reciprocal of the probability yields

$$\frac{1}{P_{f,\mathcal{BR}(z)}} \approx 1.50338537$$

, which is correct up to 3 decimal places.

We then computed approximations to $\frac{1}{P_{f,\mathcal{BR}}(z)}$ for a range of z. it does not appear the limit $P_{f,\mathcal{BR}}(z)$ converges. In fact the data once again, as in Section 2.2, suggests two different limits, $P^e_{f,\mathcal{BR}}(z)$ and $P^o_{f,\mathcal{BR}}(z)$, based on the parity of n as demonstrated below.

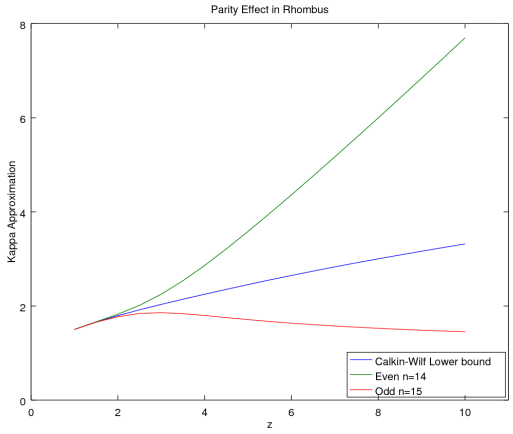

Figure 1.17: The parity effect on the rhombus radius

Once again if we compute the geometric mean of the two parities, it appears to approach $\kappa(z)$. However, the convergence is faster and more definite for means where the larger parity is even.

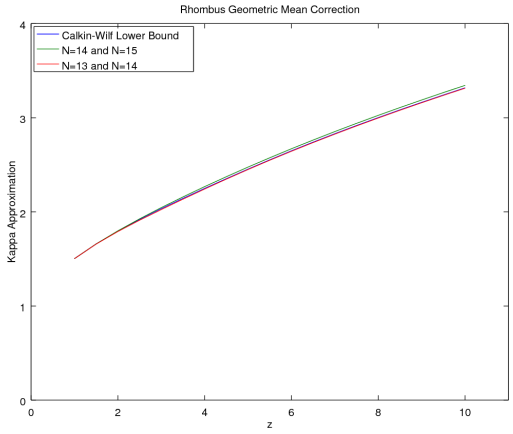

Figure 1.18: The means appear to be consistent with Calkin and Wilf

Further, if we apply a checkerboard boundary, the expression $\sqrt{\frac{z}{P_{c,\mathcal{BR}}(z)}}$, where $P_{c,\mathcal{BR}}(z)$ is the probability of the origin being a 1, appears to approach $\kappa(z)$.

The checkerboard boundary is only meaningful for even n, as for odd n the origin is forced to be a 0. Below is a graphic of the checkerboard boundary condition applied for $n = 2$. As we can see, the majority of the boundary is composed of 0's.

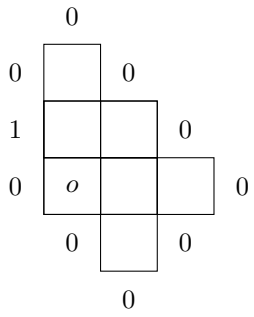

Figure 1.19: The checkerboard boundary for a broken rhombus

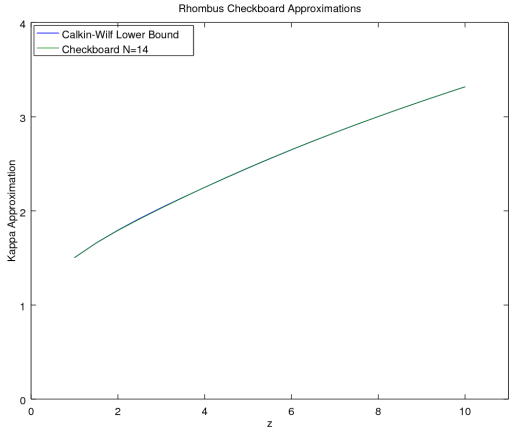

Figure 1.20: The checkerboard boundary appear to be consistent with Calkin and Wilf

2.6 Linear System

Since $\lim_{n\to\infty} Z_n(z)^{\frac{1}{n^2}} = \kappa(z)$, we expect that $Z_n(z) \approx \kappa(z)^{n^2}$ for sufficiently large n. Additional correction terms may be applied to $\kappa(z)^{n^2}$ in order to better approximate $Z_n(z)$. Our "ansatz", or guess as to what these correction terms should be is

$$Z_n(z) = A(z)\kappa(z)^{n^2}\rho(z)^n \tag{1.22}$$

Our ansatz is based on physical intuition. There are $(n-2)^2$ squares in an $n \times n$ box which do not touch its boundary, and hence the function $\kappa(z)$ should reflect the "bulk" behaviour in $Z_n(z)$. There are then about $4n$ squares which are touch its boundary, and hence we call $\rho(z)$ are "surface pressure" term and refers to the effect of the boundary on $Z_n(z)$. Finally $A(z)$ is a "corner" term and reflects any behaviour in $Z_n(z)$ which is subexponential, since there are a constant number of "corner" vertexes.

Based on the ansatz, we may linearize it by taking logarithms:

$$\log Z_n(z) = \log A(z) + n^2 \log \kappa(z) + n \log \rho(z) \tag{1.23}$$

By adding two additional equations to 1.23, we may form a 3×3 system of linear equations to solve for $A(z), \kappa(z)$ and $\rho(z)$ since we may compute $Z_n(z)$ for each z of interest. Suppose we add the following two equations:

$$\log Z_{n-1}(z) = \log A(z) + (n-1)^2 \log \kappa(z) + (n-1) \log \rho(z) \tag{1.24}$$

$$\log Z_{n-2}(z) = \log A(z) + (n-2)^2 \log \kappa(z) + (n-2) \log \rho(z) \tag{1.25}$$

We then calculate approximations $A(z), \kappa(z), \rho(z)$ using $n = 4$ all the way to $n = 14$. Then as n increases, the solutions for $\kappa(z), A(z), \rho(z)$ converge for small z, appear to be different between even and odd n for sufficiently large z.

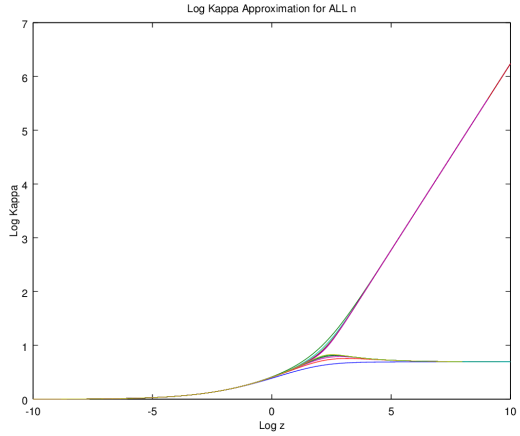

Figure 1.21: Solution for $\kappa(z)$ is bounded for even n but unbounded for odd n

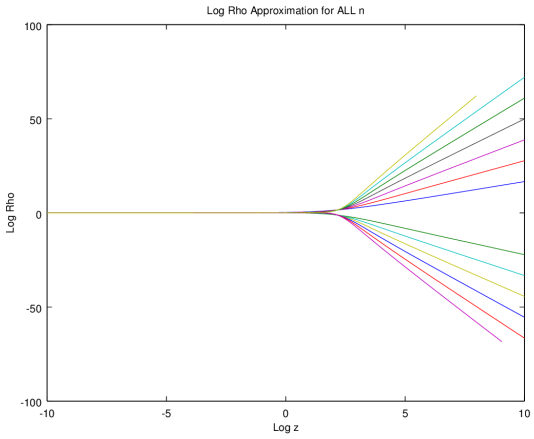

Figure 1.22: Solution for $\rho(z)$ tends to $+\infty$ for even n but tends to $-\infty$ for odd n

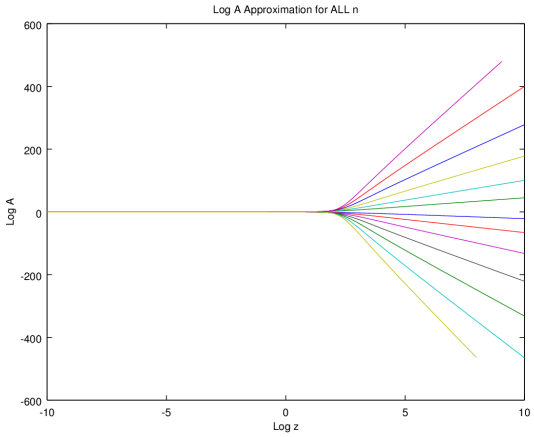

Figure 1.23: Solution for $A(z)$ tends to $-\infty$ for even n but tends to $+\infty$ for odd n

The divergence in the odd and even solutions for sufficiently large z is another expression of the "parity effect" as mentioned in Section 2.2 as the sitewise probability of seeing a "0" differs between the odd sites and the even sites. In order to correct for parity, we instead add:

$$\log Z_{n-2}(z) = \log A(z) + (n-2)^2 \log \kappa(z) + (n-2) \log \rho(z) \tag{1.26}$$

$$\log Z_{n-4}(z) = \log A(z) + (n-4)^2 \log \kappa(z) + (n-4) \log \rho(z) \tag{1.27}$$

Upon adding 1.23 and 1.27 to form a system of linear systems to solve the functions in question, approximations for $\kappa(z), \rho(z)$ converge for free boundary conditions. Additionally we may use $Z_n^{\omega}(z)$ for some boundary condition ω and approximate $A(z), \kappa(z), \rho(z)$ for those conditions. Boundary conditions may include checkboard boundary conditions, as discussed in Section 2.3, but also cylindrical boundary conditions by imposing that the first and last columns are compatible. Tordial boundary conditions means cylindrical boundary conditions and also imposing that the first and last rows be compitable. The values $n = 13$ and $n = 14$ were used to obtain these approximations to $A(z), \rho(z), \kappa(z)$ for all such boundary conditions.

All approximations to $\kappa(z)$ converged and are consistent with each other. This is because all boundary conditions ω may be expressed in terms of the free boundary condition, as mentioned in Section 2.4.

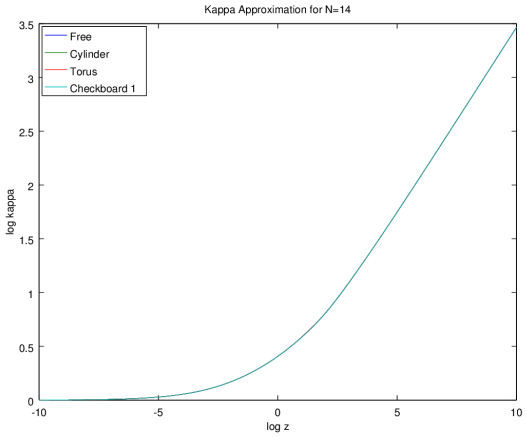

Figure 1.24: Approximations to $\kappa(z)$ obtained using linear system approach

Approximations to $\rho(z)$ display a more interesting pattern. The approximations converge under free or checkboard boundary condition. However, there is a parity effect for cylindrical or tordial boundary conditions, wherein as $z \to \infty$ $\rho(z) \to 1$ for even n whereas $\rho(z) \to 0$ for odd n.

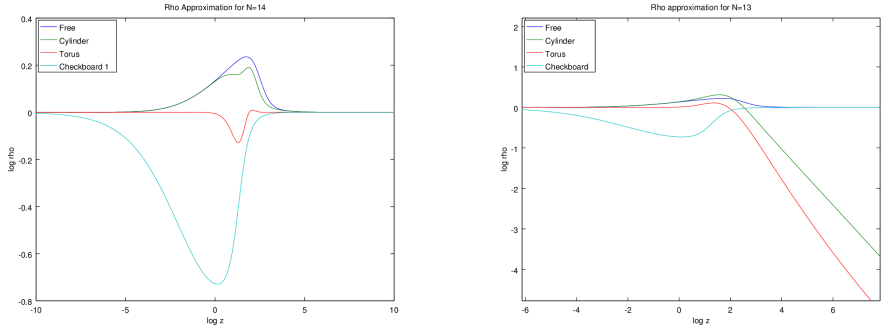

Figure 1.25: Approximations to $\rho(z)$ obtained using linear system approach, displaying parity effect in cylindrical and tordial boundary conditions. Even is on the left, odd is on the right.

Approximations to $A(z)$ continue to display parity effects under all boundary conditions, even when the parity correction 1.27 is applied. In all cases, the even parity yields a bounded solution, but $A(z) \to +\infty$ in the odd parity for all conditions except the checkboard condition (where $A(z) \to 0$).

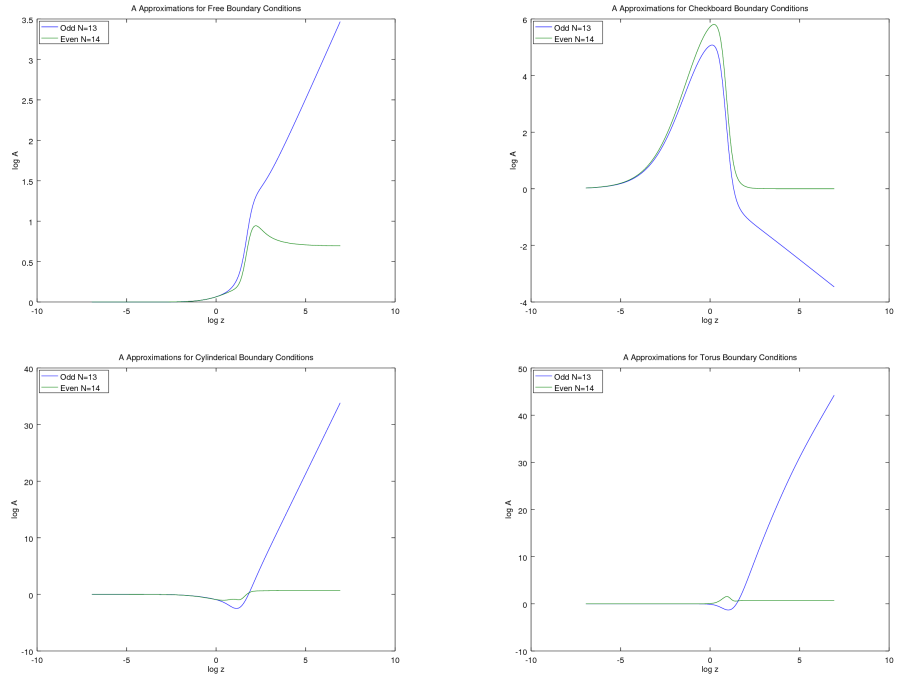

Figure 1.26: Approximations to $A(z)$ obtained using linear system approach, displaying parity effect under all boundary conditions. Top left is free, top right is checkboard, bottom left is cylinder, bottom right is torus. Blue is odd, green is even.

This may indicate that our "ansatz" is wrong when dealing with the corner pressure term.

2.7 Series Expansions

The free energy $\kappa(z)$ and related functions $\rho(z)$ and $A(z)$ as defined in Section 2.6 currently do not have known closed-form expressions. However, these functions may be expanded into an infinite series for certain ranges of z in order to study their properties for such z. In this research, series expansions are used to get more rigorous estimates for $\kappa(z), \rho(z), A(z)$ in comparison with the methods in Section 2.6 consistent and to add additional evidence for believing that Conjecture 2 in Section 2.3 is true.

Correction Terms

The first few terms of $Z_{nn}(z)$, the partition function for general $n \times n$ hard squares, can be computed by "graph counting" arguments. The coefficient of z^i in $Z_{nn}(z)$ denotes the number of hard square configurations with i "1"s on an $n \times n$ box. This coefficient is a polynomial in n. We obtained, with the aid of computer software, that

$$Z_{nn}(z) = 1+n^2z+\frac{1}{2}n(n-1)(n^2+n-4)z^2+\frac{1}{6}(n-2)(n^5+2n^4-11n^3-10n^2+42n-12)z^3+O(z^4) \tag{1.28}$$

We may use the same anstaz in Section 2.6, that $Z_{nn}(z) = A(z)\kappa(z)^{n^2}\rho(z)^n$ in order to "fit" a series for $A(z), \kappa(z), \rho(z)$. Assuming that $A(z), \kappa(z), \rho(z)$ can be expanded into a series, we may plug the series into the right hand side of the ansatz, then match the right hand side with 1.28 to obtain series coefficients for $A(z), \kappa(z), \rho(z)$. Once this process is complete, we get

$$\kappa(z) = 1 + z - 2z^2 + 8z^3 + ... \tag{1.29}$$

$$\rho(z) = 1 + 2z^2 - 16z^3 + ... \tag{1.30}$$

$$A(z) = 1 + 4z^3 + ... \tag{1.31}$$

We expect such series to converge for $|z| < 0.12$, as Chan in [8] noted that there is a dominant, non-physical singularity of $\kappa(z)$ at approximately -0.12.

The following are ranges of z for the series "works". The error is defined as the difference between the truncated series and the numeric approximation given using the linear system.

Series	Range s.t. Error < 0.001	Range s.t. Error < 0.01
$\kappa(z)$	(0, 0.0797)	(0, 0.149)
$\rho(z)$	(0, 0.0604)	(0, 0.117)
$A(z)$	(0, 0.0797)	(0, 0.159)

The above data is consistent with our estimated radius of convergence. We also plot the functions $\kappa(z), \rho(z), A(z)$ in the ranges in which the numeric and the series approximate each other within 0.01, as seen below.

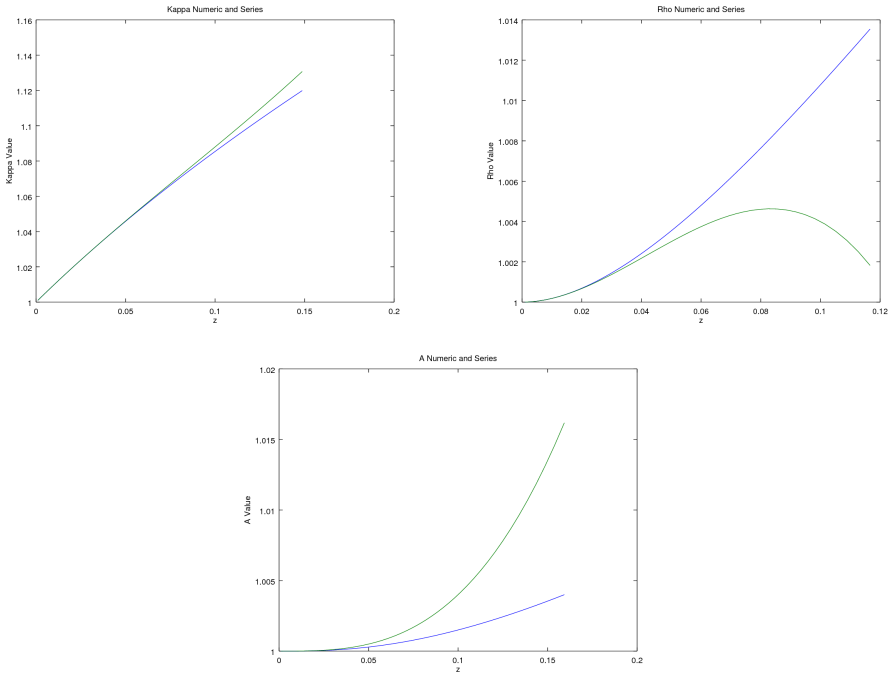

Figure 1.27: Plot of numerics obtained and series obtained for $\kappa(z)$ (top left), $\rho(z)$ (top right), and $A(z)$ (bottom centre) for free boundary conditions around $z = 0$

The techniques above may be useful in determine the leading order behaviour of free energy, surface pressure, and corner pressure functions, in general.

Checkboard Series

Chan in [8] and [9] had obtained series expansions for $\kappa(z)$ via the method of corner transfer matrices, one of which is a "low z" expansion and the other of which is a "high z" expansion. Due to phase transitions in $\kappa(z)$, we would expect the "low z" expansion to work for $|z| < 0.12$.. and the high z expasion to work for $|z| > 3.79$.... Let $\gamma(z) = \frac{1}{P_{c,\mathcal{B}}(z)}$. Since there is a relationship between $\kappa(z)$ and $\gamma(z)$, namely:

$$\gamma(z) = \frac{\kappa(z)^2}{z} \tag{1.32}$$

We may use the expansions for $\kappa(z)$ in [8] and [9] to obtain expansions for $\gamma(z)$. We calculated 8 terms for $\gamma(z)$ in both the high z and low z regimes.

For low z, we get that

$$\gamma(z) = \frac{1}{z} + 2 - 3z + 12z^2 - 60z^3 + 338z^4 - 2050z^5 + 13076z^6... \tag{1.33}$$

For high z, we get that

$$\gamma(z) = 1 + \frac{1}{z} + \frac{1}{z^3} - \frac{1}{z^4} + \frac{5}{z^5} - \frac{10}{z^6} + \frac{39}{z^7} - \frac{95}{z^8}... \tag{1.34}$$

Observe that the series coefficient for $\gamma(z)$ are alternating in sign except for the first few terms. The alternating sign property enables rigorous estimates for the error between the truncated series and the actual value of $\gamma(z)$.

The truncated series of 8 terms $\gamma_{8 \text{ terms}}(z)$, which approximates $\gamma(z)$, was compared with another approximation, $\gamma_{\text{box}}(z)$ for $\gamma(z)$, namely the inverse probability of seeing a "1" at the origin on a $16 \times 30 \times 30$ box. The comparison is a way to measuring how good a truncated series approximates numerically computed probability functions.

The following table gives the approximate ranges of z for which the relative error $E(z) = \frac{|\gamma_{8 \text{ terms}}(z) - \gamma_{\text{box}}(z)|}{\gamma_{8 \text{ terms}(z)}}$ is below a certain value in the low z regime. Relative error was chosen since $\gamma(z) >> 1$ for low z.

	10^{-1}	10^{-2}	10^{-3}	10^{-4}
Low z Expansion	(0, 0.154)	(0, 0.113)	(0, 0.0825)	(0, 0.0625)

The observations match our hypothesis at the series converges for approximately $|z| < 0.12$. Next, the following table gives the approximate ranges of z for which the absolute error $E(z) = |\gamma_{8 \text{ terms}}(z) - \gamma_{\text{box}}(z)|$ is below a certain value in the high z regime.

	10^{-1}	10^{-2}	10^{-3}	10^{-4}
High z Expansion	(2.070, ∞)	(2.828, ∞)	(4.0000, ∞)	(5.278, ∞)

Notably the error between the series and the numerics are relatively low much earlier than $z > 468$, which was the range for which 1.32 was proven to hold in [10]. The computed error between the numerics and the series by $z = 468$ is less than the machine epsilon, and hence the computer registers the error as "0". Hence, we have additional evidence for believing that Conjecture 2 in Section 2.3 is true.

Low and high z series, along with the numeric values of $\gamma(z)$ were plotted in the following graph. It can be seen that there is a range of z in which neither series seems to be a good approximation.

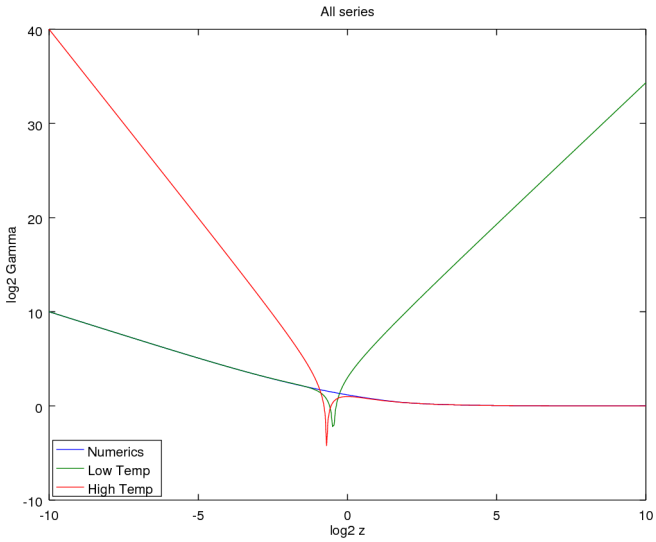

Figure 1.28: All approximations for $\gamma(z)$

Furthermore, in the above analysis, we have two proxies for $\gamma(z)$, namely a truncated series for the function along with numeric approximations to it computed using a finite-width box. We may expand the box, or add more terms to the series, in order to obtain better approximations to $\gamma(z)$. In this analysis, we chose to vary the number of series terms. The error between $\gamma_{\text{box}}(z)$ and truncated series of $5, 6, 7, 8$ terms is plotted below.

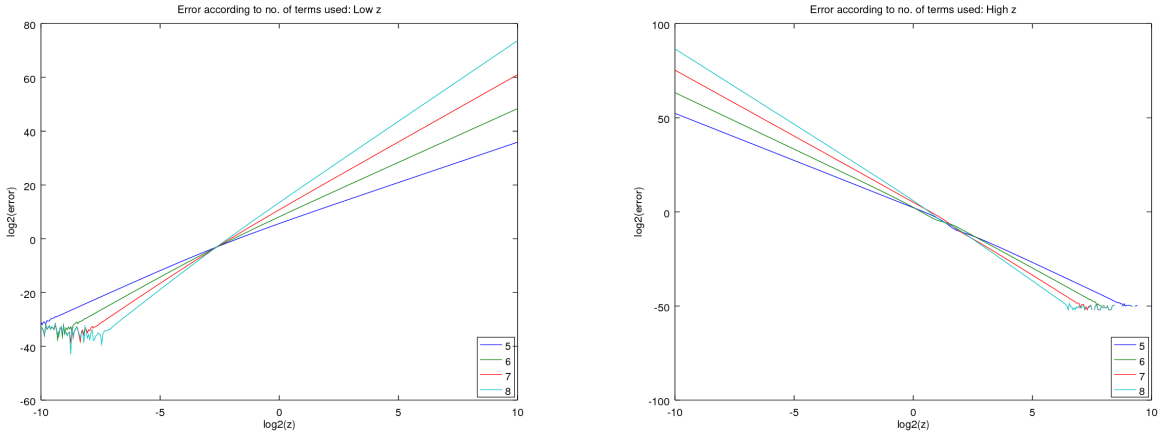

Figure 1.29: Term by term error between $\gamma_{\text{box}}(z)$ and truncated series

It is visible from the figures that there is a radius of convergence z_c of the series, at which the series diverges for all $z \geq z_c$ in the low z case and for all $z \leq z_c$ in the high z case.

We may also try expanding the box in order to see if bigger boxes yield "better" approximations to $\gamma(z)$ than using additional terms of the series beyond 8 terms. A rigorous analysis of the rate of convergence of the numeric approximations and series approximations to $\gamma(z)$, in order to compare them, may also be possible but difficult.

In summary, we have a number of methods to approximate $\kappa(z)$, and the following are the values we obtain when approximating $\kappa(10)$.

Method	Relevant Parameters	$\kappa(10)$ Value
Calkin-Wilf Lower Bound	$\Lambda_{20,10}, \Lambda_{19,10}$	3.31801717090024...
Calkin-Wilf Upper Bound	$\xi_{20,10}$	3.31804721565178...
Geometric Mean, Free Broken Box	$17 \times 40 \times 40$ and $17 \times 41 \times 41$ box	3.317857394...
Geometric Mean, Free Broken Rhombus	$N = 14, 15$	3.3438552919...
Geometric Mean, Free Broken Rhombus	$N = 13, 14$	3.3136422998 ...
Checkboard Broken Box	$17 \times 40 \times 40$ box	3.3180464659...
Checkboard Broken Rhombus	$N = 14$	3.3180464502...
Linear System	$N = 16$	3.31808917987507...
High z Series	8 terms	3.31804603644977...

Table 1.3: Summary of $\kappa(10)$ values computed using different methods

Conclusion

1 Summary of Work Done

Our work has explored hard square model using computational methods as outlined in Sections 2.1-2.3 and Sections 2.5-2.7. The result of our work was a computational framework to perform calculations about hard squares, and additionally, novel conjectures about the behaviour of the growth rate $\kappa(z)$ as it relates to probability functions on a broken box or broken rhombus. We also conducted a number of investigations on how methods in [3] extend to computing $\kappa(z)$ in general, needed corrections to $\kappa(z)$ in order to approximate $Z_n(z)$, and a series expansion for $\gamma(z)$. Some of results from these investigations provide additional evidence for our main conjectures.

2 Future Directions

There are a number of additional questions or research directions we would like to propose based on our summer research.

The first direction is one which is theoretical. There are a number of conjectures we have related to the broken box probability functions with either free or checkboard boundary conditions in Section 2.2 and Section 2.3. Computational evidence as outlined in Section 2.2 and 2.3 seem to indicate that the conjectures are true. Attempting to prove the conjectures seems like a reasonable next step, although it may be quite difficult and use complex machinery.

The second direction is one which is experimental or computational. We had explored a broken rhombus in Section 2.5 in order to get a lattice which somehow "maximizes" a parity effect. During meetings, it was proposed that "broken triangle" lattice in which columns have monotonically increasing, then decreasing widths, would also achieve such an effect although we did not have time to implement code to explore this suggestion. The next computational experiment we could do is related to the site-wise building up of configurations as mentioned in Section 2.4. We had noted in some computational experiments that the site-wise probability of seeing a '1" changes as the number of sites in the lattice increases. More work needs to be done to examine rigorously these effects.

The third direction is based on work related in series in Section 2.7 in order to analytically get at some of the quantities of interest including functions $\kappa(z), \rho(z), A(z)$ and $\gamma(z)$. Firstly, we can extend the graph counting arguments in Section 2.7 to find $Z_n(z)$ given checkerboard, cylindrical or tordial boundary conditions. Given such $Z_n(z)$ and the methods of "fitting series", we can obtain more rigorously the quantities $\kappa(z), \rho(z), A(z)$ for such conditions beyond a numeric approximation given using methods in Section 2.6. Graph counting can also be used to get a "high z" expansion for $\kappa(z), \rho(z), A(z)$. This involved finding an expression for $Z_n(z)$ based on starting with a checkerboard and taking off symbols one by one, then fitting the series. This

may be useful in understanding the behaviour of these terms for high z. Next, it may be useful to exploit the alternating series for $\gamma(z)$ in order to obtain rigorous bounds for how well the a truncated series approximates the function $\gamma(z)$.

Finally, we are interested in how the methods used throughout this report can be extended to different models. Some additional "nearest neighbour" constraints on $\mathbb{Z}^2$ such as the non-attacking kings and read-write isolated memory model are described in [7], and we are curious to see how the computational methods used in this report can be used to study these models. We are also interested in furthering our study of statistical mechanics in general, as models such as the Ising-Potts models and colouring models piqued our interest earlier in the project.

Bibliography

[1] D. Lind and B. Marcus. *An Introduction to Symbolic Dynamics and Coding.*

[2] R.J. Baxter, I.G. Enting, and S.K. Tsang. *Hard Square Lattice Gas*

[3] N. J. Calkin and H. S. Wilf. *The Number of Independent Sets in a Graph*

[4] K. Engel. *On the Fibonacci Number of a $m \times n$ Lattice*

[5] S. Friedland, P. H. Lundow and K. Markstörm. *The 1-Vertex Transfer Matrix and Accurate Estimation of Channel Capacity*

[6] Y. Chan and A. Rechnitzer. *Accurate Lower Bounds on Two-Dimensional Constraint Capacities from Corner Transfer Matricies*

[7] Y. Chan and A. Rechnitzer. *Upper Bounds on the Growth Rate of Hard Squares and Related Models via Corner Transfer Matricies*

[8] Y. Chan. *Series Expansions from the Corner Transfer Matrix Renormalization Group Method: The Hard Square Model*

[9] Y. Chan. *Series Expansions from the Corner Transfer Matrix Renormalization Group Method: II. Asymmetry and High Density Hard Squares*

[10] S. Adams, R. Briceño, B. Marcus, R. Pavlov. *Representation and poly-time approximation for pressure of $\mathbb{Z}^2$ lattice models in the non-uniqueness region*

[11] J.C. Vera, E. Vigoda, L. Yang. *Improved bounds on the phase transition for the hard-core model in 2-dimensions.*